ORIGINAL ARTICLE

Myc target gene, long intergenic noncoding RNA, *Linc00176* in hepatocellular carcinoma regulates cell cycle and cell survival by titrating tumor suppressor microRNAs

DDH Tran[1], C Kessler[1], SE Niehus, M Mahnkopf, A Koch and T Tamura

Hepatocellular carcinoma (HCC) is a frequent form of cancer with a poor prognosis and with limited possibilities for medical intervention. Recent evidence has accumulated that long noncoding RNAs (lncRNAs) are important regulators of disease processes including cancer. Chromatin remodeling in cancer cells may result in an unusual expression of lncRNAs and indeed it has been shown that more than 7000 unannotated lncRNAs are expressed in HCCs. We identified a novel long intergenic noncoding RNA, *Linc00176*, that plays a role in proliferation and survival of HCC. *Linc00176* regulates expression of more than 200 genes by the sponge function for tumor suppressor miRNAs, miR-9 and miR-185. *Linc00176* is expressed at a high level only in HCC, and is activated by Myc, Max and AP-4 transcription regulators. Myc also upregulates miR-9 and miR-185. In *Linc00176*-depleted HCC, these miRNAs were released from *Linc00176* and downregulated their target mRNAs. Thus, depletion of *Linc00176* disrupted the cell cycle and induced necroptosis in HCC via released tumor suppressor miRNAs. These data indicate that atypically expressed lncRNAs may be useful targets for cancer therapy.

Oncogene (2018) **37,** 75–85; doi:10.1038/onc.2017.312; published online 4 September 2017

INTRODUCTION

Hepatocellular carcinoma (HCC) is one of the most prevalent tumor types worldwide;[1] however current treatment options are limited and there are no precise and effective medical strategies.[2] Furthermore, biopsies for HCC diagnosis and biomarkers[3] are of limited use. Risk factors for HCC such as viral infection, alcoholic liver injury or steatohepatitis may lead to chronic hepatitis or cirrhosis (preneoplastic stages);[2] however, the molecular mechanisms by which HCC further develops are largely unknown. It has been recently shown by exome sequencing of HCC that 161 putative driver genes are associated with 11 recurrently altered pathways in HCC development.[4] These facts suggest that multiple target molecules will be required for effective HCC therapy. Notably, these same authors found that 28% of altered gene products are involved in a chromatin-remodeling complex, suggesting that HCC expresses unique genes that are not expressed in normal hepatocytes.

The comprehensive expression analysis of the ENCyclopedia of DNA Element (ENCODE) project found that 60–70% of the bases in the human genome could be found in transcripts, while among these only approximately 1.5% of the genome code for proteins.[5,6] Noncoding RNAs have molecular functions across cellular pathways and processes, including oncogenic signaling. In particular, some noncoding RNAs, such as long intergenic RNA (lincRNA) or microRNA exhibit the regulatory potential in coding RNA expression and play roles in cancer formation. Moreover, recently 58 648 genes were classified as long noncoding RNA (designated MiTranscriptome lncRNA),[7] indicating that the number of long noncoding RNAs is 2–3-fold greater than protein coding RNAs.

Furthermore, 8603 lncRNAs have been recently identified using RNA-seq data from 20 HCC patients.[8] Notably, approximately 76% of the lincRNAs identified in the HCC samples were not annotated by the MiTranscriptome, indicating that the expression of lncRNAs is highly cell type and cancer type specific. These noncoding regulatory RNAs modify the expression of their target gene by suppression of transcription, mRNA stability, as well as modified translation and post-translational modification;[9] however, the molecular and cellular functions of the majority of long noncoding RNAs remain unknown.

We have recently shown that THOC5, a member of TREX (transcription/export), is expressed in HCC at an enhanced level.[10] The depletion of THOC5 in HCC cell lines, Huh7 and HepG2, caused downregulation of 396 genes and those cells then underwent apoptosis, suggesting that THOC5 target genes play a role in survival of HCC. Therefore, we further studied the role of THOC5 target genes in HCC maintenance.

In this study we have characterized one of these *THOC5* target genes, *Linc00176*. *Linc00176* is activated by Myc and is expressed at high levels in HCC, but not in normal liver or other type of tumor cell lines. Strikingly, depletion of *Linc00176* caused downregulation of 144 genes and as a result HCC ceased to proliferate and underwent necroptosis. *Linc00176* binds several tumor suppressor miRNAs and inhibiting these miRNAs partially rescued *Linc00176*-depleted cells from cell cycle inhibition and cell death. Moreover, *Linc00176* is expressed in primary HCCs at high levels, suggesting that *Linc00176* participates in HCC development by inhibiting tumor suppressor miRNAs.

Institut fuer Biochemie, OE4310, Medizinische Hochschule Hannover, Hannover, Germany. Correspondence: Professor T Tamura, Institut fuer Biochemie, OE4310, Medizinische Hochschule Hannover, Carl-Neuberg-Str. 1, D-30623 Hannover, Germany.
E-mail: Tamura.Teruko@MH-Hannover.de
[1]These two authors contributed equally to this work.

RESULTS

Linc00176 is expressed at high levels exclusively in HCC

We recently showed that the depletion of THOC5 in HCC cell lines, HepG2 and Huh7, causes apoptosis.[10] Simultaneously, a number of THOC5 target genes were downregulated (GEO series: GSE70178), suggesting that some of these genes play an important role in survival of HCC. One of the THOC5 target genes is *Linc00176*, a gene that has not been well characterized.[10] We first analyzed the features of a *Linc00176* transcript in HCC. *Linc00176* (NR_027686.1) is located on chromosome 20, 62665697–62671315 (5.619 kb long, GRCh37), contains four exons and three introns and its transcript is 5264 nucleotides long

(Figure 1a). The RNA-Sequence (RNA-seq) data generated by the ENCODE Consortium[5] revealed that *Linc00176* in HepG2 cells does not contain Exon 1 (E1), but contains parts of Exon 2 (E2a: 1705–1894; E2b: 3495–3770, all numbers are nucleotide (nt) numbers). Notably, the 3′-end E2a contains a potential 5′ splice site 'atg**GT**gagcag' and the 5′-end of E2b contains a potential 3′ splice site 'tgtctcctcc**AG**gta' (Figure 1a, blue circles).[11] Furthermore, *Linc00176* in HepG2 contains Exon 3 (E3) and Exon 4 (E4) that is 962 nt shorter than NR_027686.1 (Figure 1a, E4a: 3924-4302). Here, the E4a contains a typical polyadenylation signal sequence 'AATAAA' at positions 4273–4278, while E4b (4303–5264) does not contain any typical polyadenylation signal sequence[12] at 3′-end (NR_027686.1). Importantly, the *Linc00176* transcript was
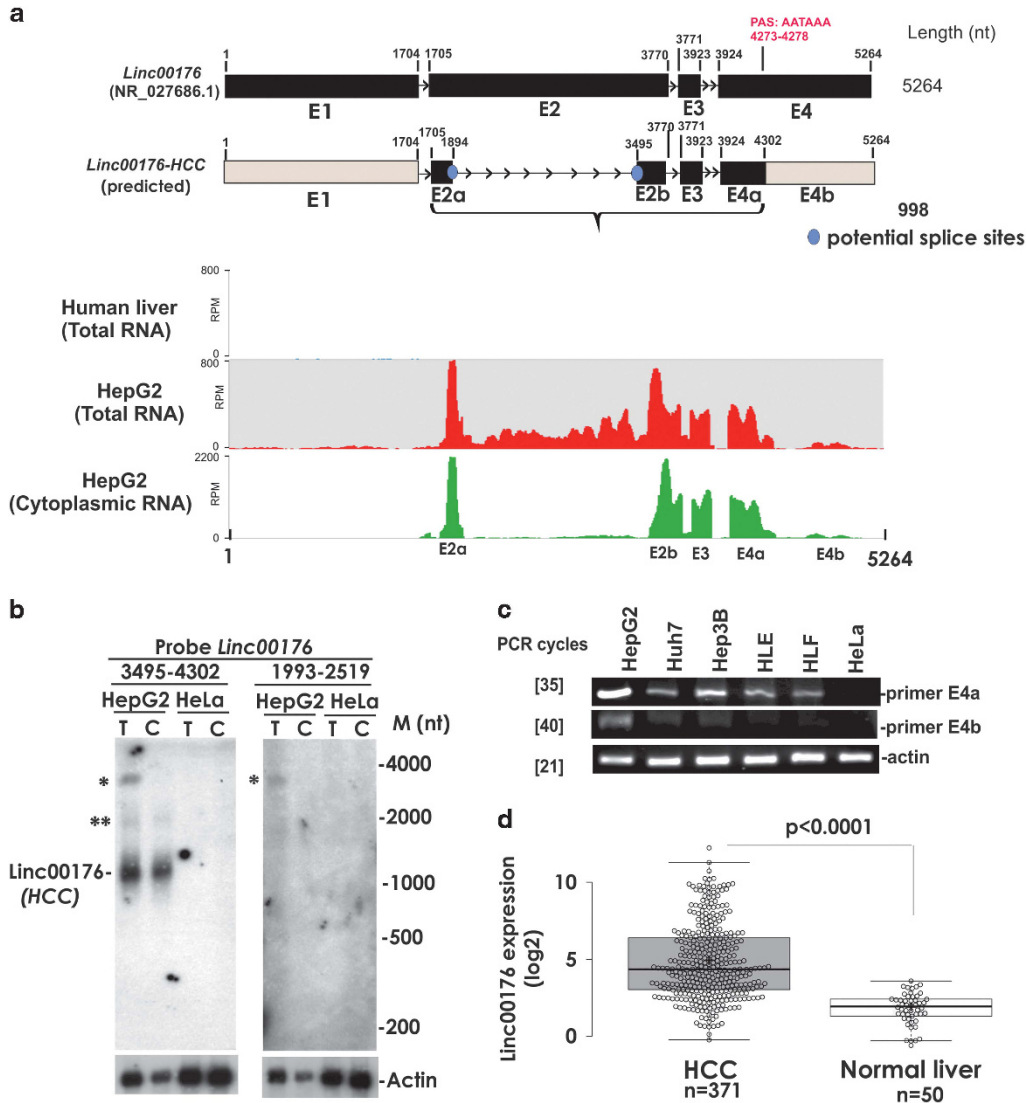

Figure 1. Truncated form of *Linc00176* is expressed exclusively in HCC. (**a**) Scheme of *Linc00176* (NR_027686.1) and predicted *Linc00176* that is expressed in HepG2 cells (*Linc00176-HCC*). Closed blue circles represent potential splice sites (1894 and 3495) in Exon 2 (E2a: 1705–1894; E2b: 3495–3770). Exon 4 (E4a: 3924–4302; E4b: 4303–5264), '4273–4278' exhibits typical polyadenylation signal (PAS) site for 3′ cleavage (in red). Black boxes: expressed at high levels; gray boxes: expressed at low levels in HCC. Numbers represent nucleotide number. Total RNA-seq data sets from human liver tissue (ENCFF184YUO) and HepG2 cells (ENCFF834ITU) and cytoplasmic RNA-seq from HepG2 cells (ENCFF337WTM) generated by the ENCODE Consortium were aligned to the reference human genome (hg19). SeqMonk was used to quantitate and visualize the data. Blue, red and green peaks in the wiggle plot represent the normalized RNA-seq read coverage on *Linc00176*. RPM, reads per million. (**b**) *Linc00176*-specific northern blot analysis. Total (T) and cytoplasmic (C) PolyA+RNAs were isolated from HepG2 or HeLa cells and analyzed by northern blot using *Linc00176* probes (3495–4302 and 1993–2519, numbers are the nucleotide numbers from relative to transcriptional start) and actin probes. (**c**) RNAs were isolated from HepG2, Huh7, Hep3B, HLE, HLF and HeLa cells and supplied for *Linc00176* E4a (4049–4291), E4b (5064–5262) and Actin-specific semiquantitative RT–PCR. [ ]: PCR cycles. (**d**) Expression of *Linc00176* in 371 primary HCC and 50 normal liver samples. Data obtained from the cancer genome atlas (TCGA) (https://cancergenome.nih.gov/) shown as box blot. *P*-value: *t*-test between total 371 HCCs and 50 normal liver.
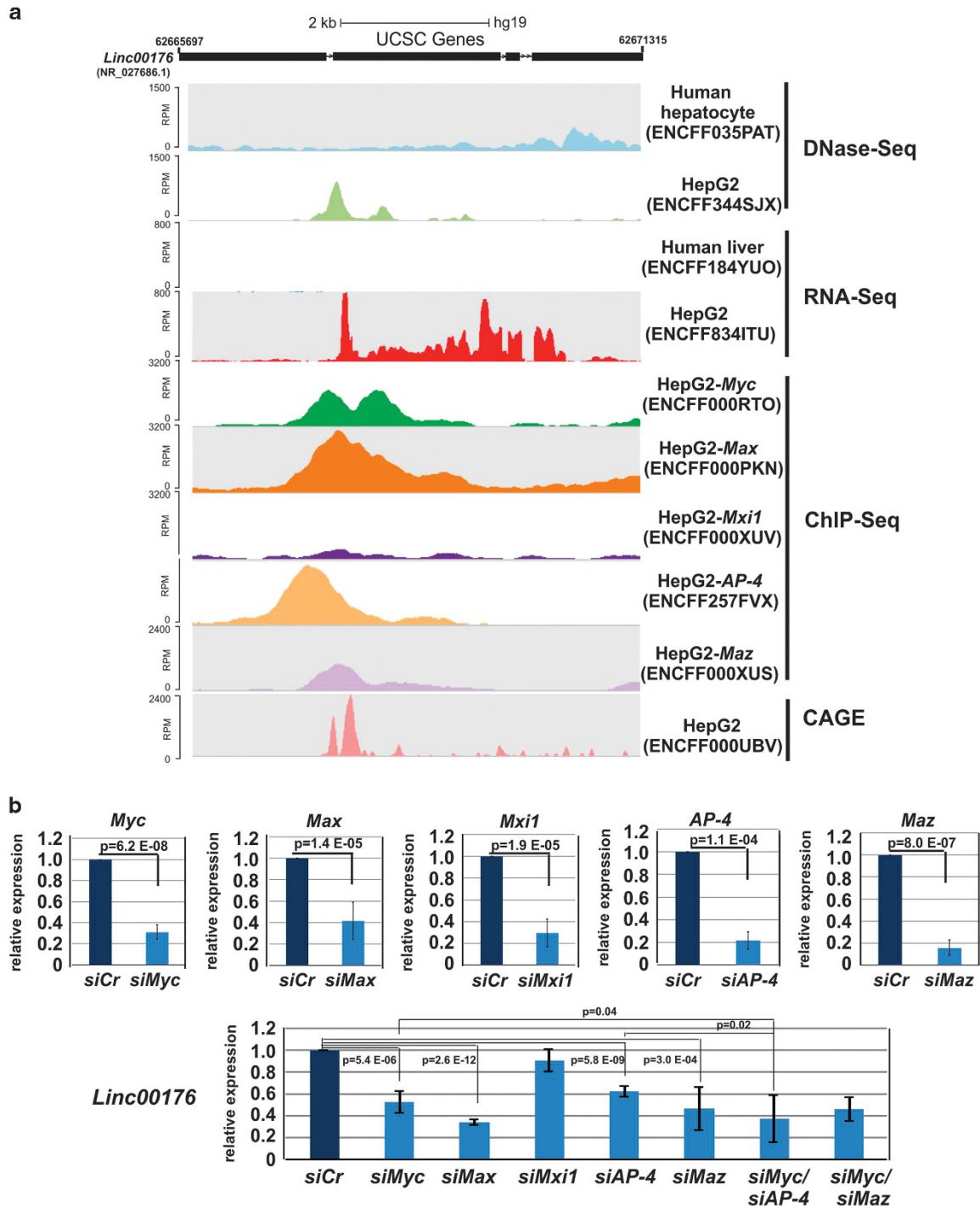
Figure 2. Myc/Max regulates the expression of *Linc00176*. (**a**) DNase-sequencing (DNase-seq) data sets from human hepatocytes (ENCFF035PAT) and HepG2 (ENCFF344SJX), total RNA-seq data sets from human liver tissue (ENCFF184YUO) and HepG2 cells (ENCFF834ITU), ChIP-seq data sets from HepG2 *Myc* (ENCFF000RTO), HepG2 *Max* (ENCFF000PKN), HepG2 *Mxi1* (ENCFF000XUV), HepG2 *AP-4* (ENCFF257FVX) and HepG2 *Maz* (ENCFF000XUS), and cap analysis of gene expression (CAGE) data in HepG2 cells (ENCFF000UBV) generated by the ENCODE Consortium were aligned to the reference human genome (hg19). SeqMonk was used to quantitate and visualize the data. (**b**) siCr (control 1) and si*Myc, siMax, siMxi1, siAP4* and/or si*Maz* were transfected in HepG2 cells and RNA was applied for *Myc, Max, Mxi1, AP4, Maz* or *Linc00176*-specific qRT–PCR. Three independent experiments were performed. Numbers are mean $\pm$ 95% CI. *P*-value: *t*-test.

exported to the cytoplasm (cytoplasmic RNA-Seq, ENCFF337WTM) (Figure 1a). In agreement with these data, northern blot analysis using whole and cytoplasmic RNAs isolated from HepG2 cells revealed that the probe containing E2 (1993–2519) hybridized with only 3 kb transcript in the total RNA, but not in a cytoplasmic sample (Figure 1b). However, the probe containing E2b–E3–E4a

(3495–4302) hybridized with 3 (Figure 1b) and 1 kb transcripts from total RNA and in the cytoplasmic RNA fraction only 1 kb transcript was detected, suggesting that a part of E2 is spliced in the nucleus and the E2a–E2b–E3–E4a transcript (998 nt long) is exported to the cytoplasm (Figure 1a). It should be noted that a weak band with 2 kb was detected in HepG2 cells in both fractions

(**), suggesting that some transcripts may contain E4b portion. *Linc00176* is expressed at a low level or is not transcribed in normal human liver (ENCFF184YUO) or in other type of human organs and cells, namely pancreas (ENCFF070UKL), heart (ENCFF331CGL), B-cell (ENCFF496ACN), skin (ENCFF969GXB), lung (ENCFF202ETQ), temporal brain lobe (ENCFF460PJA), muscle
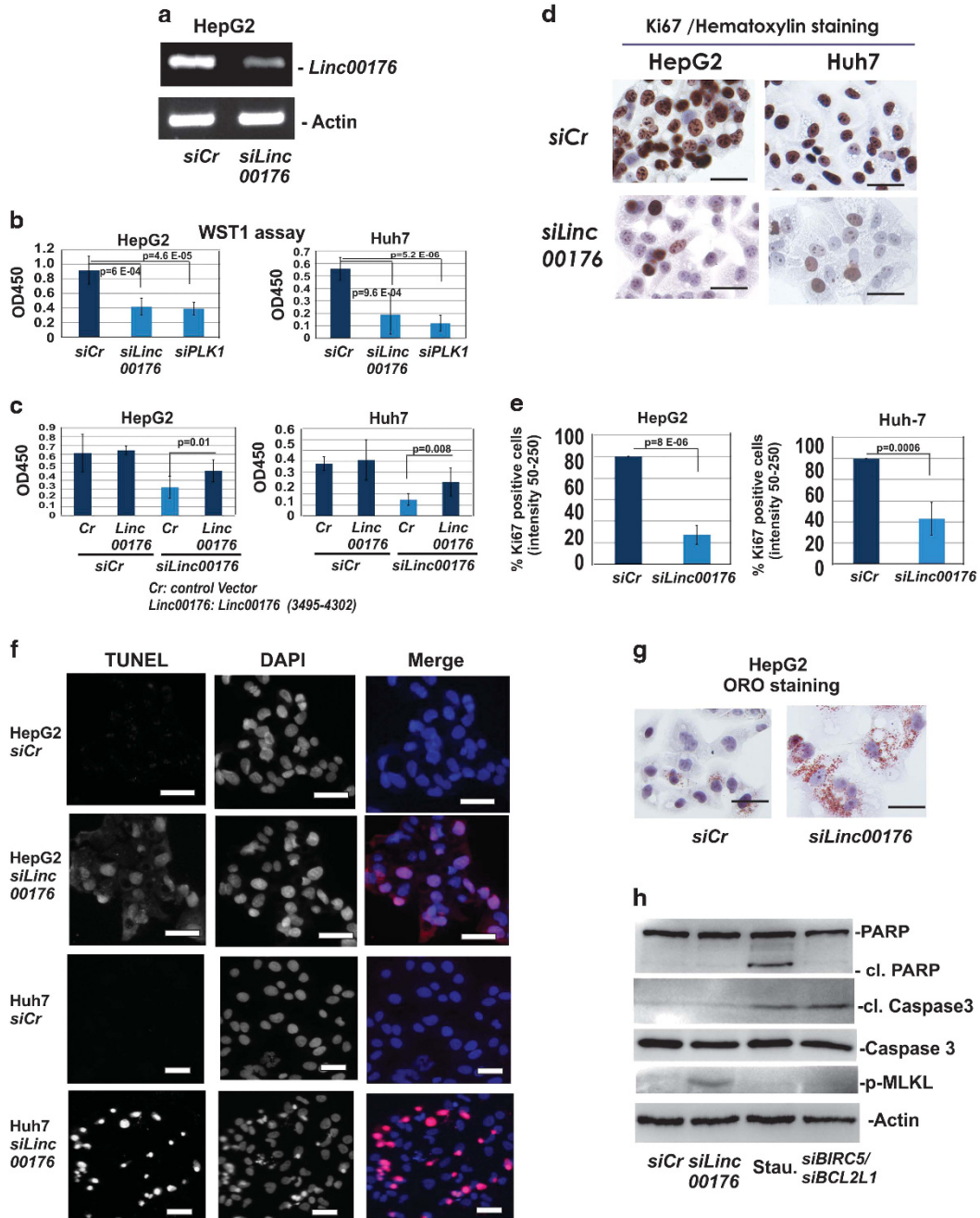

Figure 3. Depletion of *Linc00176* causes inhibition of cell cycle and induced necroptosis. (**a**) RNA was isolated from HepG2 cells 2 days after transfection with siCr or si*Linc00176* and applied to *Linc00176* or actin-specific RT–PCR. (**b**, **c**) WST assay using an *siCr*- and si*Linc00176*-transfected HepG2 and Huh7 cells were performed. As positive control *siPLK1*-transfected cells were applied (**b**). A sister culture from (**b**) were transfected with Sport6 plasmid (Cr) or with the same plasmid carrying *Linc00176 (3495–4302)* (*Linc00176*) and 3 days after transfection WST assay was performed (**c**). Mean of OD_{450} value is shown and four independent experiments were performed. Numbers are mean ± 95% CI. (**d**) Same preparation was stained with Ki67-specific antibody by the IHC technique. Representative images are shown. Bars represent 50 μm. (**e**) To quantitate the intensity of *Ki67* staining, reciprocal pixel intensity was determined by subtracting *Ki67* intensity from the maximum pixel intensity in white unstained area (as measured by the mean intensity function in the Nikon NIS elements D 3.0 Software). The mean percentage from 6 (HepG2) or 4 (Huh7) experiments of dark staining (dark: reciprocal intensity 50–250) nuclei is shown ± 95% CI. At least 200 cells from three images were quantitated per experiment. *P*-value: *t*-test. (**f**, **g**) Three days after siCr or si*Linc00176* transfection cells were stained with DAPI and TUNEL (**e**) or Oil Red O and hematoxylin (**f**). Bars represent 50 μm. Representative images were shown. The experiments were independently performed four times. (**h**) HepG2 cells were transfected with siCr, si*Linc00176* or si*Birc5/siBCL2L1*. Three days after transfection cell extracts were supplied for PARP, caspase 3, cleaved caspase 3 (Cl. Caspase 3), phopho-MLKL (p-MLKL) and actin-specific immunoblot. As positive control cells were treated with 5 μM Staurosporine (Stau.) for 24 h. The experiments were independently performed three times.

(ENCFF422EVZ), mesenchymal Wharton's Jelly (ENCFF124IFE), mesenchymal adipose (ENCFF272UGL), mesenchymal bone marrow (ENCFF568GFK), H7-hESC (ENCFF823RHH) or other type of cancer cell lines, such as K562 (ENCFF340LGI), A375 (ENCFF295KHF), MCF-7 (ENCFF451FWL), SK-N-DZ (ENCFF104SFV), SJCRH30 (ENCFF764MHS) or HeLa (ENCSR552EGO). We next examined the *Linc00176* transcript in several human cell lines, such as HepG2, Huh7, HLE, HLF and HeLa using two sets of PCR primer pairs E4a (4049–4291) and E4b (5064–5262). *Linc00176* is expressed in HepG2 at the highest level among these cell lines, however, is also expressed in all HCC cell lines, Huh7, Hep3B, HLE and HLF (Figure 1c). Using primer pair E4b (5064–5262), the amount of reverse transcriptase–PCR (RT–PCR) product was much less than the product from primer pair E4a (4049–4291) in all cell lines (Figure 1c). These data again suggest that *Linc00176-HCC* (E2a–E2b–E3–E4a) (Figure 1a) is expressed in HCC. Notably, *Linc00176* E1 (1034–1329) was also slightly transcribed in both HepG2 and Huh7, but to a much lesser extent (Supplementary Figure S1). We next examined the *Linc00176* expression in primary human HCCs. In agreement with data obtained from HCC cell lines, the cancer genome atlas (TCGA) data (https://cancergenome.nih.gov/) reveals that significantly enhanced levels of *Linc00176* expression (*P*-value < 0.0001) were found in primary HCCs (*n* = 371) compared with normal control liver (*n* = 50) (Figure 1d).

Linc00176 is regulated by Myc/Max and AP-4 transcription regulators

Since *Linc00176* is expressed at high levels only in HCC, we next studied how *Linc00176* is regulated. We examined the chromatin structure at the *Linc00176* putative promotor region using DNase-sequencing data (DNase-seq) generated by the ENCODE Consortium.[5] DNase-seq data (Figure 2a) obtained from human hepatocyte (ENCFF035PAT) and HepG2 (ENCFF344SJX) in *Linc00176* gene reveals that HepG2 contains DNase I hypersensitive sites at the proximal region of the 5′-end of E2 of *Linc00176-HCC*, while human normal hepatocytes do not contain these sites at this position (Figure 2a), suggesting that the chromatin structure in this region is remodeled in HCC cells. To define the transcription initiation site, we utilized the cap analysis of gene expression (CAGE) data in HepG2 cells (Figure 2a, ENCFF000UBV). In agreement with RNA-seq data, the cap site is located at the 5′-end of E2 (Figure 2a). *Linc00176-HCC* putative promotor region (500 nt upstream from the initiation site) contains 78 transcription regulator binding sites predicted by PROMO (ALGGEN). Among these, 36 factors are expressed in HepG2 and 9 transcription regulators may be involved in cancer formation. Of these, Myc, Maz, AP-4, c-Jun, c-Fos, and JunD specific ChIP-seq data from HepG2 are available in ENCODE. Myc, Maz and AP-4 bind to this region (Figure 2a), while *c*-Jun, c-Fos and JunD do not. Furthermore, Max (a positive regulator of Myc), but not Mxi1 (a negative regulator of Myc),[13] binds to putative Linc00176 promotor region. In agreement with CHIP-seq data (Figure 2a), upon depletion of Myc, or Max the expression level of *Linc00176* is downregulated by 50% and 65%, respectively; however, upon depletion of Mxi1 the level of Linc00176 is not significantly altered (Figure 2b). Furthermore, upon depletion of AP-4 or Maz the expression level of *Linc00176* is also downregulated by 40% and 50%, respectively (Figure 2b). The depletion of transcription regulators, Myc/AP-4, synergistically downregulated the *Linc00176* expression level (Figure 2b), suggesting that Myc/Max,[13] AP-4 and Maz participate in *Linc00176* expression. Notably, it has been shown that *AP-4* is one of the Myc target genes.[14] In addition, it is also known that Maz is one of the regulators of *Myc* gene expression.[15] Indeed, upon depletion of Maz *Myc* is downregulated by 50% (Supplementary Figure S2), indicating that the effect of Maz on *Linc00176* expression is partially indirect.

Depletion of *Linc00176* inhibits cell proliferation and induces necroptosis in HCC

To examine whether *Linc00176* is involved in HCC proliferation and/or survival, we treated HepG2 and Huh7 cells with siLinc00176 (siLinc00176E4a). Upon transfection with *siLinc00176*, the level of *Linc00176-HCC* was reduced to approximately 20% (Figure 3a). Strikingly, depletion of *Linc00176* in HepG2 and Huh7 cells significantly reduced the proliferation rate within 2 days (Figure 3b, WST-1 assay, *P* = 6-E4, and *P* = 4.6-E5, respectively). To define the dynamic range of the assay, polo kinase 1 (PLK1)[16] was depleted in HepG2 and Huh7 cells and a WST-1 assay was performed. As expected, the depletion of PLK1 reduced proliferation in both cells, and the proliferation rate in these cells was not significantly different from Linc00176-depleted cells (Figure 3b). Conversely overexpression of *Linc00176* (3495–4302, nucleotide numbers) in HepG2 and Huh7 partially rescued the proliferation rate (Figure 3c, *P* = 0.01 and *P* = 0.008, respectively). Moreover, proliferation marker, Ki67, positive cells were also drastically reduced in both cell lines (Figures 3d and e, *P* = 8.0 E-6 (HepG2); *P* = 0.0006 (Huh7)).

Within 3 days both HepG2 and Huh7 cells became TUNEL positive (Figure 3f), and lipid droplets had accumulated (Figure 3g, Oil Red O). However, the depletion of Linc00176 did not cause cleavage of caspase 3 or Poly-(ADP-ribose) polymerase (PARP) in HepG2 (Figure 3h). Although treatment with apoptosis inducer Staurosporine (5 μM) caused the cleavage of PARP and caspase 3 within 24 h, the depletion of Birc5 (survivin) and BCL2L1 induced only cleavage of caspase 3 in HepG2 cells (Figure 3h). Since the necroptosis marker, mixed lineage kinase-like (MLKL) was clearly phosphorylated (Figure 3h) in *Linc00176*-depleted HepG2 cells, these cells may undergo necroptosis rather than apoptosis.[17,18] Notably, MLKL was not phosphorylated in strauroporine-treated or Birc5/BCL2L1-depleted cells (Figure 3h).

The expression level of *Linc00176* is correlated both with the differentiation grade in primary HCCs and with the survival time of HCC patients

We next examined the correlation between *Linc00176* expression and the HCC differentiation grade in primary HCCs using TCGA. The expression level was slightly correlated with the differentiation grade (normal liver to HCC (G1): *P* < 0.0001; HCC G1 to G3: *P* = 0.08) (Figure 4a).

Importantly, the *Linc00176* expression level is also significantly correlated with HCC patient survival time. We analyzed data using Kaplan–Meier estimation. Correlation between Linc00176 expression level (log2 RSEM (RNA-Seq by Expectation-Maximization) ⩾ 5 (*n* = 37): log2 RSEM < 5 (*n* = 52)) and survival time (within 700 days) is significant (Figure 4b, log rank test: *P* = 0.026). These data suggest that *Linc00176* participates in growth and/or survival of HCC in cell lines as well as in primary HCCs.

Depletion of *Linc00176* downregulates 144 genes within 24 h

To examine whether *Linc00176* is one of the regulatory RNAs, we performed transcriptome analysis using RNA isolated from HepG2 transfected with *siLinc00176* or siCr RNA. Strikingly 24 h after transfection, 144 genes were downregulated (>2-fold) and 66 genes were upregulated (>2-fold) (Figure 5a and Supplementary Tables S1 and S2, GEO series: GSE93548). Among these genes 126 downregulated and 59 upregulated genes were recognized by Ingenuity Pathways analysis (version 23814503) (Qiagen, Hilden, Germany). Ingenuity Pathways analysis reveals that the top of category 'disease' is cancer (*P* = 1.21E-02–3.94 E-05) and the top category 'molecular and cellular function' is cell cycle (1.21E-02–6.12E-07). Notably, 40 genes were involved in cell cycle. Among these 40 genes, 20 genes were involved in the M-phase, 6 genes in G2/M and 5 genes in G2 phase (Figure 5a). Furthermore, the
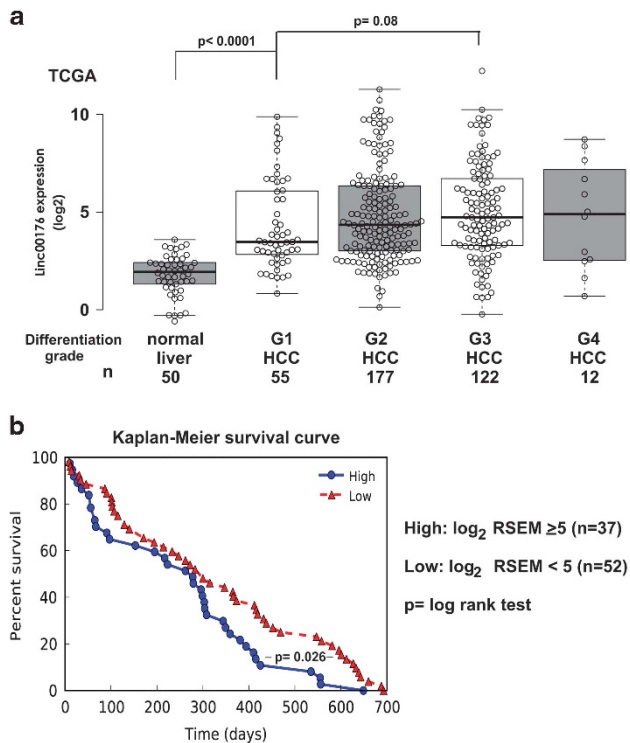
a

b

Figure 4. Expression level of *Linc00176* is correlated to differentiation grade in primary HCCs and survival time of HCC patient. (**a**) Expression of *Linc00176* in differentiation grade G1–G4 HCC and normal liver ($n = 50$) samples. Data obtained from the cancer genome atlas (TCGA) (https://cancergenome.nih.gov/) shown as box blot. *P*-value: *t*-test between total G1 HCCs and 50 normal liver and G1 and G3 HCC. (**b**) Correlation between Linc00176 expression level (log$_2$ RSEM (RNA-seq by expectation-maximization) $\geqslant 5$ ($n = 37$): log$_2$ RSEM < 5 ($n = 52$)) and survival time (within 700 days) is shown using Kaplan–Meier estimation (Log rank test: $P = 0.026$).

category 'liver necrosis/cell death' showed clear significance ($P = 8.25$ E-04–1.5E-04) in the upregulated gene pool, including peroxisome proliferator activated receptor alpha (*PPARA*) and selenoprotein P (*SEPP1*) (Figure 5a). The upregulation of these genes after depletion of *Linc00176* was confirmed by RT–PCR (Figure 5b). We then validated some of the downregulated genes that are involved in the M-phase by qRT–PCR. As shown in Figure 5c, amphiregulin (*AREG*), sapiens Bloom syndrome, RecQ helicase-like (*BLM*), Ki67, kinesin family member 14 (*KIF14*), kinetochore scaffold 1 (*KNL1*), NDC80 kinetochore complex component (*SPC25*), and G2 checkpoint kinase (*WEE1*) genes were significantly downregulated after depletion of *Linc00176*. In addition, a potential HCC marker gene, aquaporin 11 (*AQP11*), was also a *Linc00176* dependent gene. Similar data were obtained when we applied other control siRNA and two siRNA target Linc00176 (Supplementary Figure S3).

Linc00176-HCC forms a complex with Argonaute 2 (Ago2) and miRNAs

Linc00176-HCC was detected chiefly in the cytoplasm (Figures 1a and b) and had an influence on the expression of more than 200 mRNAs (Figure 5), suggesting that *Linc00176-HCC* may titrate miRNAs (miRNA sponge). Since *Linc00176-HCC* is co-immunoprecipitated with Argonaute 2 (Ago2), a major protein in RNA-induced silencing complex (RISC)[18] (Figure 6a), we examined potential miRNA binding sites in *Linc00176-HCC* using the program MIRANDA 3.3a (parameters: Score 140, energy -7, scale 7)[19] by screening with 544 high confidence microRNAs (https://www.mirbase.org). We then selected miRNAs according to

the following criteria. (1) potential tumor suppressor microRNAs having more than 15 binding sites to *Linc00176*. (2) microRNAs that express > 8 RPM (reads per million) in HepG2 cells (miRmine database and ENCODE:ENCFF000JGU). Six miRNAs, namely miR-9-5p,[20] miR-16-5p,[21] miR-29a-3p,[22] miR-31-5p,[23] miR-152-3p[24] and miR-185-5p,[25] belong to this category. To select further miRNAs that participate in the role of *Linc00176* in HCC, inhibitors of these miRNAs were transfected in HepG2 cells and 24 h later the level of *Linc00176* expression was examined by qRT–PCR. Depletion of miR-9-5p, miR-152-3p and miR-185-5p, but not miR-16-5p, miR-29a-3p and miR-31-5p, upregulated the expression level of *Linc00176* (> 1.5-fold) (Figure 6b), suggesting that these miRNAs may play a role in *Linc00176* dependency of HCC. To examine the direct interaction between *Linc00176* and these miRNAs, we generated pMS2-TRAP (MS2-tagged RNA purification, a kind gift from Dr Myriam Gorospe) and *Linc00176* (3495–4302) fusion gene, pMS2-TRAP-*Linc00176*.[26] Two miRNAs, miR-9 and miR-185, but not miR-152, were bound specifically to MS2-TRAP-*Linc00176* complex, but not to MS2-TRAP (Figure 6c).

The expression of miR-9 and miR-185 is regulated by Myc

The TCGA data show that the expression level of tumor suppressor miRNAs, miR-9 and miR-185, but not miR-152, is significantly higher in HCC than in normal liver control (Figure 6d, $P = 8.4E-05$ and $P = 3.2E-07$, respectively). To analyze transcriptional regulation of these miRNAs we again utilized ChIP-seq data from HepG2 (ENCODE consortium).[5] ChIP-seq data revealed that Myc/Max binds at the putative promoter of miR-9 and miR-185 (Supplementary Figure S4), but not of miR-152. Indeed, upon depletion of Myc the expression of both miR-9-5p and miR-185-5p, but not for miR-152-3p, was significantly downregulated ($P = 0.008$ and $P = 0.0002$, respectively) (Figure 6e). Furthermore, pre-miR-9 and pre-miR-185 were also significantly downregulated ($P = 8E-05$ and $P = 4E-04$, respectively) upon depletion of Myc (Figure 6e). These data indicated that *Linc00176* (pro-tumor), miR-9-5p (anti-tumor) and miR-185-5p (anti-tumor) are upregulated by Myc; however, *Linc00176* absorbed these miRNAs and HCC proliferate. Thus, the *Linc00176* dependency of HCC may be due to the increased level of tumor suppressor miRNAs. To confirm this hypothesis, we examined whether the treatment with inhibitors of miR-9 and/or miR-185 rescued *Linc00176*-depleted HCC from cell death.

Treatment with inhibitors of miR-9-5p and miR-185-5p rescues *Linc00176*-depleted HCC from cell death

HepG2 and Huh7 cells were transfected with siCr and siLinc00176 in the presence or absence of inhibitors of miR-9 (miR-9-5p In), miR-152 (miR-152-3p In) and/or miR-185 (miR-185-5p In). In the presence of inhibitors of miR-9-5p or miR-185-5p, but not of miR-152-3p, the number of Ki67-positive cells were increased in *Linc00176*-depleted HepG2 and Huh7 (Figure 7a). Furthermore, treatment with both miR-9/185 inhibitors synergistically increased the number of Ki67-positive cells (Figure 7a). Simultaneously TUNEL-positive cells were no longer seen in siLinc00176-depleted HCC (Figure 7b). Upon depletion of both miR-9 and miR-185, all genes were significantly upregulated (*Ki67*: $P = 5E-05$, *KIF14*: $P = 0.0004$, *KNL1*: $P = 0.002$, *SPC25*: $P = 0.0006$). Notably, 80% of *AQP11* gene expression was recovered by the treatment with miR-185-5p inhibitor alone in *Linc00176*-depleted cells. Here, the *AQP11* gene contains a binding site for miR-185-5p with high score. These data strongly suggest that *Linc00176* plays a role in HCC proliferation and survival via titration of tumor suppressor microRNAs, including miR-9 and miR-185 (Figure 7d).
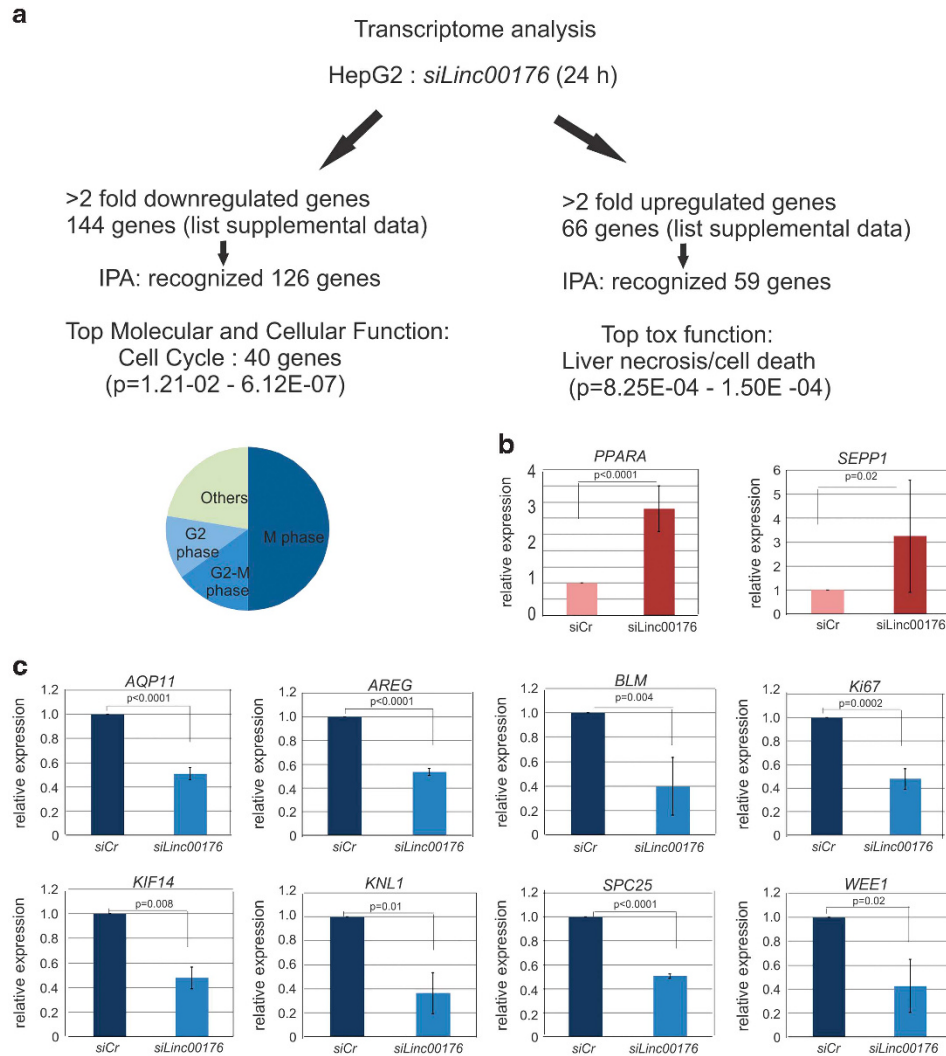
Figure 5. Upon depletion of *Linc00176* in HepG2, 144 genes are downregulated within 24 h. RNAs were isolated from HepG2 cells transfected with siCr or si*Linc00176* 24 h after transfection. Using these RNA samples, dual-color microarray experiments were performed based on the Agilent platform. The complete microarray data along with processing protocols have been deposited in NCBI′s Gene Expression Omnibus and are accessible through GEO series accession number GSE93548. (**a**) Down- and upregulated genes were analyzed by Ingenuity Pathway Analysis (IPA: version 23814503). Diagram of 40 downregulated genes (>2-fold) that are involved in G2, G2–M, M, or other cell cycle phases. (**b**, **c**) Validation of transcriptome analysis data. *PPARA, SEPP1* (**b**, upregulated genes) *AQP11, AREG, BLM, Ki67, KIF14, KNL1, SPC25* and *WEE1* (**c**, downregulated genes) specific qRT–PCR using RNAs from HepG2 cells transfected with siCr or si*Linc00176* was performed. Primer pairs for each PCR are described in Supplementary Table S3. Numbers are mean ± 95% CI. Three independent experiments were performed. *P*-value: *t*-test.

DISCUSSION

Evidence has accumulated that exquisite regulation of lincRNA transcription can provide signals of malignant information.[6] LincRNAs drive many important cancer phenotypes through their interactions with other cellular macromolecules including DNA, protein and RNA.[6,9] Since regulatory RNAs such as lincRNA or miRNA regulate a subset of genes, targeting these RNAs induces a much greater effect on cancer cells than targeting single gene.

Here we show that targeting *Linc00176* altered the expression of 210 genes and induced HCC cell death. Since normal liver does not express *Linc00176,* the question arises as to why *Linc00176* is required for survival of HCC, but not of normal hepatocytes? Our working hypothesis was: (1) When normal hepatocytes are transformed, chromatin remodeling occurs. Here, DNase-seq data revealed that chromatin at the putative promotor region of *Linc00176* is opened in HCC but not in normal hepatocytes. In this context, it has been shown that 28% of genetic alteration in HCC is in the chromatin remodeling gene pool.[4] (2) Since Myc is

ubiquitously expressed, Myc target gene, *Linc00176*, is activated when chromatin structure has been remodeled. In addition, Myc target gene *AP-4* also participates in further *Linc00176* gene activation. (3) Simultaneously Myc activates tumor suppressor miRNAs, miR-9 and miR-185. (4) Their target genes, such as *Ki67, KIF14, KNL1* or *SPC25* play a key role in mitosis; however, *Linc00176* absorbs these tumor suppressor microRNAs, thus allowing cancer cells to grow. (5) When *Linc00176* is depleted in HCC, enhanced levels of miR-9 and miR-185 are released and suppress genes that control mitosis. Thus, HCCs undergo cell death. HCC patient data obtained from TCGA strongly support this working hypothesis; however, it is presently not clear whether *Linc00176* plays a significant role *in vivo*. Since most lincRNAs, including *Linc00176*, are expressed only in the primate lineage but not in any other animals,[27] they are difficult to study *in vivo*. The establishment of a primate system may be useful for the *in vivo* study of these lincRNAs. However, *in vivo* study of lincRNAs may be also possible on human liver transplanted chimeric mice.
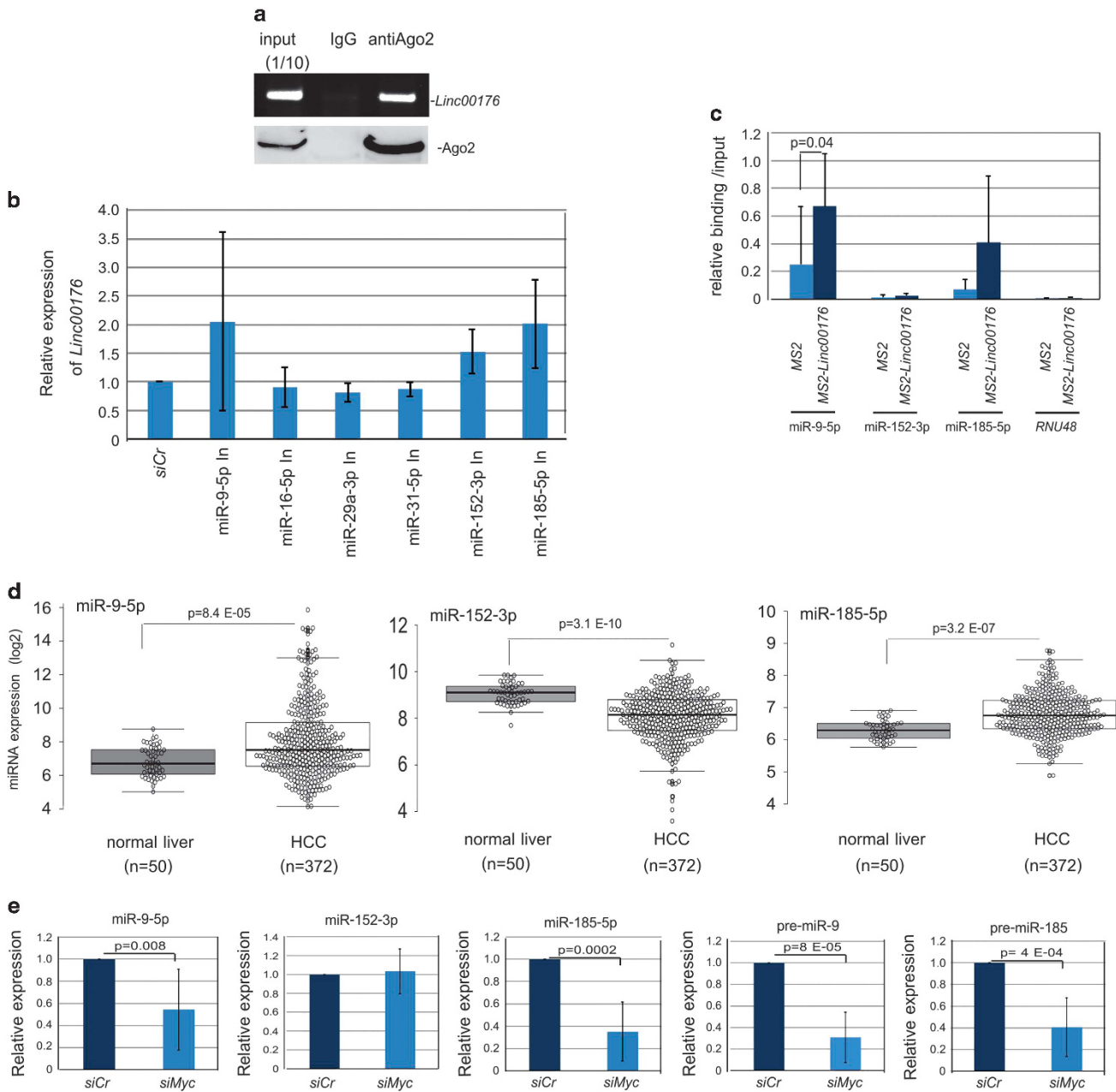
Figure 6. *Linc00176-HCC* binds to Ago2 and tumor suppressor miRNAs, miR-9 and miR-185 that are upregulated by Myc. (**a**) HepG2 cell extract was precipitated with anti Ago2 antibody or control IgG. RNA was isolated from precipitates and supplied for *Linc00176*-specific RT–PCR or immunoprecipitates were supplied for Ago2-specific immunoblot. Input: 1/10 cell lysate. (**b**) Inhibitors of miRNAs (miR-9-5p In, miR-16-5p In, miR-29a-3p In, miR-31-5p In, miR-152-3p In, miR-185-5p In) were transfected in HepG2 cells and RNAs were isolated 24 h after transfection. *Linc00176*-specific qRT–PCR was performed. Numbers are mean ± 95% CI. Three independent experiments were performed. (**c**) *Linc00176* (3495–4302, nucleotide number) was fused to MS2 using MS2-TRAP vector (MS2-*Linc00176*). pMS2-TRAP or pMS2-TRAP-*Linc00176* were transfected with GST-MS2 binding vector in HEK293 cells. After isolation of MS2-*Linc00176* by glutathione Sepharose-bound miRNAs were analyzed by qRT–PCR. Relative binding to input (1.0) is shown. Four independent experiments were performed. RNU48 (SNORD48 small nucleolar RNA, C/D box 48) as a negative control. (**d**) Expression of miR-9, miR-152 and miR-185 in 372 primary HCC and 50 normal liver samples. Data obtained from the cancer genome atlas (TCGA) (https://cancergenome.nih.gov/) show as box blot. *P*-value: *t*-test between total 372 HCCs and 50 normal livers. (**e**) siCr and si*Myc* were transfected in HepG2 cells and miR-9, pre-miR-9, miR-152, miR-185 and pre-miR-185 specific qRT–PCR was performed. Numbers are mean ± 95% CI. Three independent experiments were performed. *P*-value: *t*-test.

Although miR-9[20] and miR-185[25] have been shown to be tumor suppressor miRNAs, expression levels of these two microRNAs are significantly higher in HCC than in normal control liver. In agreement with our data, miR-9 has been shown to play a tumor suppressor role in HCC,[20,28] miR-9 is upregulated in advanced pathological stages and has an influence on the prognosis of the disease.[29–31] Noncoding regulatory RNAs such as *Linc00176* in

cancer cells may be involved in the disparity of data between the expression level of miR-9 and its functional role.

Zhu *et al.*[32] recently showed that deletion of the putative promotor region of *Linc00176* by CRISPR-Cas9 caused enhancement of Huh7 cell proliferation, suggesting that *Linc00176* participates in cell growth suppression; however, we show here that *Linc00176* instead plays a role in cell proliferation in both
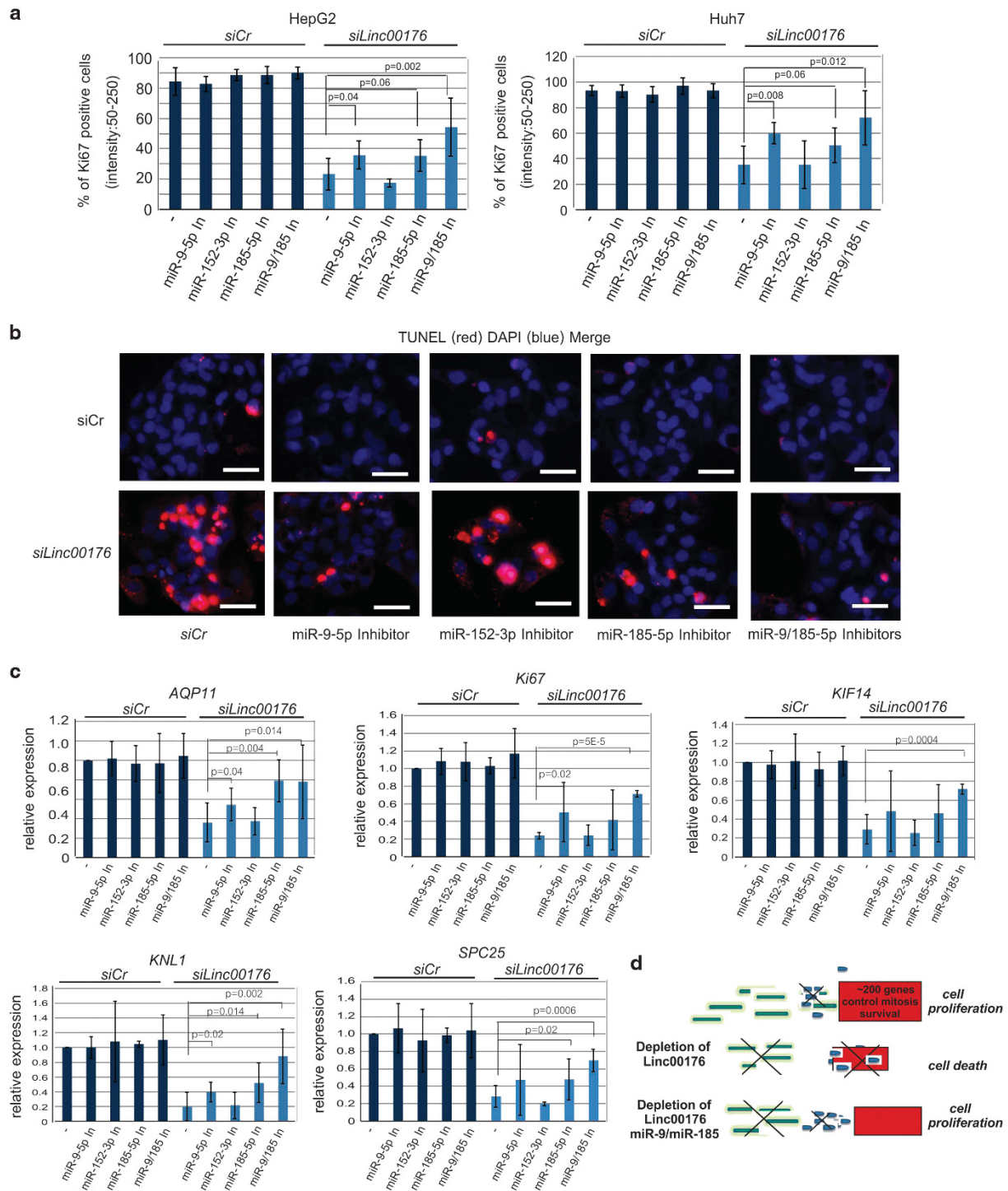
Figure 7. The treatment with inhibitors of miR-9 and miR-185 rescues *Linc00176*-depleted HCC from cell death. (**a**) HepG2 or Huh7 cells were transfected with siCr or si*Linc00176* in the presence or absence of inhibitors of miR-9 (miR-9-5p In), miR-152 (miR-152-3p In) and/or miR-185 (miR-185-5p In) and incubated for 2 days. After fixation, cells were stained with *Ki67*-specific IHC. The mean percentage from three experiments of dark staining (reciprocal intensity 50–250) nuclei is shown ± 95% CI. At least 200 cells from three images were quantitated per experiment. *P*-value: *t*-test. (**b**) Three days after *siCr* or si*Lic00176* transfection cells in the presence or absence of miRNA inhibitors as indicated were stained with DAPI (blue) and TUNEL (red). Merged representative images were shown. Bars represent 50 µm. (**c**) *AQP11, Ki67, KIF14, KNL1* and *SPC25* specific qRT–PCR using RNAs from HepG2 cells transfected with siCr or si*Linc00176* in the presence or absence of miRNA inhibitors as indicated. Primer pairs for each PCR are described in Supplementary Table S3. Numbers are mean ± 95% CI. Three independent experiments were performed. *P*-value: *t*-test. (**d**) Working hypothesis of the function of *Linc00176*. *Linc00176* inhibits the function of tumor suppressor miRNA, miR-9-5p and miR-185-5p. Therefore, the high level of *Linc00176* expression leads to stronger proliferation. By depletion of *Linc00176* high levels of tumor suppressor miRNAs are released to downregulate target genes. As a result cells stop proliferation and undergo cell death. By depletion of *Linc00176* and miR-9/miR-185, cells proliferate.

HepG2 and Huh7. This difference may be due to the location of the *Linc00176* promotor that was deleted in this work. The authors deleted chromosome 20, 62665399–62666196 (GRCh37) that is located at proximal region of *Linc00176* E1 (Promotor 1). In HepG2 cells the transcription start site pool is 62667496–62667605 (ENCSR000CJM) and two Myc binding sites in *Linc00176* located at '62667411–62667655' and '62667984–62668233' (ENCSR000DLR) that are located at the proximal region of Linc00176 E2 (Promotor 2). Moreover, it is not clear that the deletion of E1 proximal region influenced the expression level of *Linc00176* transcript in HepG2 or Huh7 cells. It may be that *Linc00176* E1 contains a negative transcriptional control element as shown in *Myc* E1.[33] We are currently analyzing this region.

It has been recently shown that the lncRNA function is highly cell type specific.[34] Using the CRISPRi approach the authors identified 499 lncRNA loci in seven cell lines required for cellular growth. Of these 89% showed a growth modifying function exclusively in one cell type. Although targeted delivery of siRNA to specific tumor tissues and cells still remains one of the key challenges in the development of RNA interference as a therapeutic application, tumor type-specific novel LincRNAs can be useful targets for cancer therapy.

MATERIALS AND METHODS

Cell culture, siRNA, miRNA inhibitor and transfection

HepG2, Huh7, Hep3B, HLE, HLF, HeLa and HEK293 cells were grown in Dulbecco's modified Eagle's medium supplemented with 10% fetal calf serum.

si*Linc00176* (sc-76260) (si*PRR17*), control siRNA-1 (sc-37007), si*Myc* (sc-29226), si*AP4* (sc-37690), were from Santa Cruz Technology (Santa Cruz, CA, USA). Additional control *siRNA-1* (5'-UAAGGCUAUGAAGAGAUAC-3'), si*Linc00176* 1 and 2 (5'-CUCGUUCUGUAGACUUGUU-3' and 5'-GGCCUCAAU AAACGGAGCU-3'), si*Max* (5'-GAAUUGUCUUGCAAGUUAA-3'), si*Mxi1* (5'-CACUUGGUUUGCUCAACAA-3'), si*Maz* (5'-GGAAAGGAGGAAGAAAUGU-3'), si*PLK1* (5'-GAAGAUCACCCUCCUUAAA-3'), si*BCL2L1* (5'-AGUGCAGUUCA GUAAUAAA-3') and si*BIRC5 (survivin)* (5'-CAACAUGGCUUUCUUUAUUU-3') were from Microsynth AG (Balgach, Switzerland). miRNA inhibitor for Hsa-miR-9-5p (miR-9-5p In), Hsa-miR-16-5p (miR-16-5p In), Hsa-miR-29a-3p (miR-29a-3p In), Hsa-miR-31-5p (miR-31-5p In), Hsa-miR-152-3p (miR-152-3p In) and Has-miR-185-5p (miR-185-5p In) were purchased from Integrated DNA Technology Germany GmbH (Munich, Germany). Fifty picomoles of each siRNA and miRNA inhibitor were transfected using Lipofectamine 2000 (Thermo Scientific, Waltham, MA, USA). For rescue experiments, Sport6 plasmid carrying Linc00176 (3495–4302) and control Sport6 plasmid were transfected using TransfeX (ATCC HB-8065TM; ATCC, Manassas, VA, USA) (Figure 2), or 25 pmol of miRNA inhibitors were transfected with siCr or si*Linc00176* using Lipofectamine 2000 (Figure 7).

TUNEL staining using *in situ* cell death detection kit (Roche Diagnostics, Mannheim, Germany) was performed according to the manufacturer's instructions. Counterstaining was performed using 4',6-diamidin-2-pheny-lindole (DAPI).

WST-1 assay

HCC cells (500–2000 cells/well) were seeded in duplicate on a 96-well plate and then transfected with siCr or si*Linc00176* and incubated for 2 days. A WST-1 proliferation assay kit (Roche Diagnostics) was employed according to the manufacturer's instructions.

Immunohistochemistry

Immunohistochemical studies were performed as detailed previously.[10] Rabbit monoclonal anti Ki67 was purchased from Thermo Scientific. To quantitate the intensity of Ki67 staining, reciprocal pixel intensity was determined by subtracting Ki67 intensity from the maximum pixel intensity in white unstained areas (as measured by the mean intensity function in the Nikon NIS elements D 3.0 Software).

Immunoblotting procedures

Details of immunoblotting have been described previously.[35] Polyclonal antibody against actin was purchased from Santa Cruz Biotechnology.

Polyclonal rabbit anti-cleaved caspase 3, caspase 3 and PARP antibodies are from Cell Signaling Technology (Cambridge, UK). Rabbit monoclonal antibody against phospho-MLKL and mouse monoclonal antibody against Ago2 are from Abcam (Cambridge, UK). Corresponding proteins were visualized by incubation with peroxidase-conjugated anti-rabbit, anti-mouse or anti-goat immunoglobulin (Santa Cruz Biotechnology) followed by incubation with SuperSignal West FemtoMaximum Sensitivity Substrate (Pierce, Rockford, IL, USA). Results were documented on a LAS4000 imaging system (GE Healthcare Bio-Sciences, Uppsala, Sweden).

Semiquantitative RT–PCR and qRT–PCR analysis

RNA was isolated from cells with the High Pure RNA Isolation kit (Roche Diagnostics) according to the manufacturer's instructions. One microgram of RNA was reverse-transcribed using oligo dT primer and the Omniscript reverse transcriptase kit (Qiagen) following the instructions provided. One-twentieth of the cDNA mix was used for real-time PCR using 10 pmol of forward and reverse primer and ORATM qPCR Green Rox kit (HighQu, Kraichtal, Germany) in a Qiagen Rotorgene machine. The levels of mRNA expression were standardized to the glyceraldehyde-3 phosphate dehydrogenase (Gapdh) or beta-Actin (Actin) mRNA level. miRNA was isolated using High Pure miRNA isolation kit (Roche Diagnostics). After polyadenylation miRNA was reverse-transcribed using oligo dT adaptor primer and the Omniscript reverse transcriptase kit and cDNA mix was used for real-time PCR. Levels of miRNA expression were standardized to RNU48. Primer pairs for each PCR are described in Supplementary Table S3.

Northern blot

Isolation of total and cytoplasmic RNAs and northern blot analysis were performed as described previously[36,37] *Linc00176*-specific probes 1993–2519 and 3495–4302 (number: nucleotide number) and actin probe were utilized. RiboReady color RNA ladder (VWR, Ameresco, Solon OH, USA) was applied as a marker.

RNP and RNA–RNA complex isolation

Ago2-*Linc00176* complex: HepG2 cells were lysed with lysis buffer (10 mM Tris, 150 mM NaCl, 1 mM PMSF, 0.4% NP40, protease inhibitor cocktail (Sigma-Aldrich, Munich, Germany), and RNase inhibitor). After centrifugation, supernatants were incubated with control IgG or anti Ago2 antibody, and then precipitated with protein G Sepharose. Bound RNAs were analyzed by RT–PCR.

Linc00176-miRNAs complex: HEK293 cells were transfected with pMS2-TRAP-*Linc00176* (3495–4302) or pMS2-TRAP with pMS2B-GST vector[26] and the cells were allowed to grow for 48 h. After three times washing, cells were lysed with lysis buffer. After centrifugation, supernatants were incubated with glutathione Sepharose (GE Healthcare) and then washed three times. All steps were carried out in the cold. Bound miRNAs were isolated with miRNA isolation kit (Roche Diagnostics) and then supplied for qRT–PCR analysis.

Statistical analysis and limitation of the study.

Cell experiments were performed in triplicate and a minimum of three independent experiments were evaluated. Data were reported as the mean value ± 95% confidence interval (95% CI). The statistical significance of the difference between groups was determined by the Student's test (two-sided). Correlation between Linc00176 expression level (log2 RSEM (RNA-Seq by Expectation-Maximization) $\geqslant 5$ ($n = 37$): log2 RSEM < 5 ($n = 52$)) and survival time (within 700 days) (Figure 4b) was determined by log rank test.[38]

Primary 371 HCC data gathering were limited to the availability from the cancer genome atlas (TCGA) data (https://cancergenome.nih.gov/).

ABBREVIATIONS

LincRNA, long intergenic noncoding RNA; HCC, hepatocellular carcinoma; *THOC5*, suppressors of the transcriptional defects of hpr1 delta by overexpression; GST, glutathione *S* transferase; DAPI, 4',6-diamidin-2-phenylindole; TUNEL, terminal deoxynucleotidyl transferase dUTP nick end labeling.

REFERENCES

1 Jemal A, Bray F, Center MM, Ferlay J, Ward E, Forman D. Global cancer statistics. *CA Cancer J Clin* 2011; **61**: 69–90.

2 Whittaker S, Marais R, Zhu AX. The role of signaling pathways in the development and treatment of hepatocellular carcinoma. *Oncogene* 2010; **29**: 4989–5005.

3 Ferrin G, Aguilar-Melero P, Rodriguez-Peralvarez M, Montero-Alvarez JL, de la Mata M. Biomarkers for hepatocellular carcinoma: diagnostic and therapeutic utility. *Hepat Med* 2015; **7**: 1–10.

4 Schulze K, Imbeaud S, Letouze E, Alexandrov LB, Calderaro J, Rebouissou S *et al.* Exome sequencing of hepatocellular carcinomas identifies new mutational signatures and potential therapeutic targets. *Nat Genet* 2015; **47**: 505–511.

5 Consortium EP, Birney E, Stamatoyannopoulos JA, Dutta A, Guigo R, Gingeras TR *et al.* Identification and analysis of functional elements in 1% of the human genome by the ENCODE pilot project. *Nature* 2007; **447**: 799–816.

6 Evans JR, Feng FY, Chinnaiyan AM. The bright side of dark matter: lncRNAs in cancer. *J Clin Invest* 2016; **126**: 2775–2782.

7 Iyer MK, Niknafs YS, Malik R, Singhal U, Sahu A, Hosono Y *et al.* The landscape of long noncoding RNAs in the human transcriptome. *Nat Genet* 2015; **47**: 199–208.

8 Yang Y, Chen L, Gu J, Zhang H, Yuan J, Lian Q *et al.* Recurrently deregulated lncRNAs in hepatocellular carcinoma. *Nat Commun* 2017; **8**: 14421.

9 Chen LL. Linking long noncoding RNA localization and function. *Trends Biochem Sci* 2016; **41**: 761–772.

10 Saran S, Tran DD, Ewald F, Koch A, Hoffmann A, Koch M *et al.* Depletion of three combined THOC5 mRNA export protein target genes synergistically induces human hepatocellular carcinoma cell death. *Oncogene* 2015; **35**: 3872–3879.

11 Padgett RA. New connections between splicing and human disease. *Trends Genet* 2012; **28**: 147–154.

12 Martin G, Gruber AR, Keller W, Zavolan M. Genome-wide analysis of pre-mRNA 3' end processing reveals a decisive role of human cleavage factor I in the regulation of 3' UTR length. *Cell Rep* 2012; **1**: 753–763.

13 Luscher B, Vervoorts J. Regulation of gene transcription by the oncoprotein MYC. *Gene* 2012; **494**: 145–160.

14 Jung P, Hermeking H. The c-MYC-AP4-p21 cascade. *Cell Cycle* 2009; **8**: 982–989.

15 Bossone SA, Asselin C, Patel AJ, Marcu KB. MAZ, a zinc finger protein, binds to c-MYC and C2 gene sequences regulating transcriptional initiation and termination. *Proc Natl Acad Sci USA* 1992; **89**: 7452–7456.

16 Deng H, Jiang Q, Yang Y, Zhang S, Ma Y, Xie G *et al.* Intravenous liposomal delivery of the short hairpin RNAs against Plk1 controls the growth of established human hepatocellular carcinoma. *Cancer Biol Ther* 2011; **11**: 401–409.

17 Remijsen Q, Goossens S, Grootjans S, Van den Haute C, Vanlangenakker N, Dondelinger Y *et al.* Depletion of RIPK3 or MLKL blocks TNF-driven necroptosis and switches towards a delayed RIPK1 kinase-dependent apoptosis. *Cell Death Dis* 2014; **5**: e1004.

18 Steitz JA, Vasudevan S. miRNPs: versatile regulators of gene expression in vertebrate cells. *Biochem Soc Trans* 2009; **37**(Pt 5): 931–935.

19 Betel D, Koppal A, Agius P, Sander C, Leslie C. Comprehensive modeling of microRNA targets predicts functional non-conserved and non-canonical sites. *Genome Biol* 2010; **11**: R90.

20 Zhang J, Cheng J, Zeng Z, Wang Y, Li X, Xie Q *et al.* Comprehensive profiling of novel microRNA-9 targets and a tumor suppressor role of microRNA-9 via targeting IGF2BP1 in hepatocellular carcinoma. *Oncotarget* 2015; **6**: 42040–42052.

21 Wu WL, Wang WY, Yao WQ, Li GD. Suppressive effects of microRNA-16 on the proliferation, invasion and metastasis of hepatocellular carcinoma cells. *Int J Mol Med* 2015; **36**: 1713–1719.

22 Zhu XC, Dong QZ, Zhang XF, Deng B, Jia HL, Ye QH *et al.* microRNA-29a suppresses cell proliferation by targeting SPARC in hepatocellular carcinoma. *Int J Mol Med* 2012; **30**: 1321–1326.

23 Kim HS, Lee KS, Bae HJ, Eun JW, Shen Q, Park SJ *et al.* MicroRNA-31 functions as a tumor suppressor by regulating cell cycle and epithelial-mesenchymal transition regulatory proteins in liver cancer. *Oncotarget* 2015; **6**: 8089–8102.

24 Dang YW, Zeng J, He RQ, Rong MH, Luo DZ, Chen G. Effects of miR-152 on cell growth inhibition, motility suppression and apoptosis induction in hepatocellular carcinoma cells. *Asian Pac J Cancer Prev* 2014; **15**: 4969–4976.

25 Qadir XV, Han C, Lu D, Zhang J, Wu T. miR-185 inhibits hepatocellular carcinoma growth by targeting the DNMT1/PTEN/Akt pathway. *Am J Pathol* 2014; **184**: 2355–2364.

26 Yoon JH, Srikantan S, Gorospe M. MS2-TRAP (MS2-tagged RNA affinity purification): tagging RNA to identify associated miRNAs. *Methods* 2012; **58**: 81–87.

27 Derrien T, Johnson R, Bussotti G, Tanzer A, Djebali S, Tilgner H *et al.* The GENCODE v7 catalog of human long noncoding RNAs: analysis of their gene structure, evolution, and expression. *Genome Res* 2012; **22**: 1775–1789.

28 Higashi T, Hayashi H, Ishimoto T, Takeyama H, Kaida T, Arima K *et al.* miR-9-3p plays a tumour-suppressor role by targeting TAZ (WWTR1) in hepatocellular carcinoma cells. *Br J Cancer* 2015; **113**: 252–258.

29 Cai L, Cai X. Up-regulation of miR-9 expression predicate advanced clinicopathological features and poor prognosis in patients with hepatocellular carcinoma. *Diagn Pathol* 2014; **9**: 1000.

30 Drakaki A, Hatziapostolou M, Polytarchou C, Vorvis C, Poultsides GA, Souglakos J *et al.* Functional microRNA high throughput screening reveals miR-9 as a central regulator of liver oncogenesis by affecting the PPARA-CDH1 pathway. *BMC Cancer* 2015; **15**: 542.

31 Sun J, Fang K, Shen H, Qian Y. MicroRNA-9 is a ponderable index for the prognosis of human hepatocellular carcinoma. *Int J Clin Exp Med* 2015; **8**: 17748–17756.

32 Zhu S, Li W, Liu J, Chen CH, Liao Q, Xu P *et al.* Genome-scale deletion screening of human long non-coding RNAs using a paired-guide RNA CRISPR-Cas9 library. *Nat Biotechnol* 2016; **34**: 1279–1286.

33 Levens D. How the c-myc promoter works and why it sometimes does not. *J Natl Cancer Inst Monogr* 2008; **39**: 41–43.

34 Liu SJ, Horlbeck MA, Cho SW, Birk HS, Malatesta M, He D *et al.* CRISPRi-based genome-scale identification of functional long noncoding RNA loci in human cells. *Science* 2017; **355**: pii:aah7111.

35 Tran DD, Koch A, Allister A, Saran S, Ewald F, Koch M *et al.* Treatment with MAPKAP2 (MK2) inhibitor and DNA methylation inhibitor, 5-aza dC, synergistically triggers apoptosis in hepatocellular carcinoma (HCC) via tristetraprolin (TTP). *Cell Signal* 2016; **28**: 1872–1880.

36 Guria A, Tran DD, Ramachandran S, Koch A, El Bounkari O, Dutta P *et al.* Identification of mRNAs that are spliced but not exported to the cytoplasm in the absence of THOC5 in mouse embryo fibroblasts. *RNA* 2011; **17**: 1048–1056.

37 Tamura T, Mancini A, Joos H, Koch A, Hakim C, Dumanski J *et al.* FMIP, a novel Fms-interacting protein, affects granulocyte/macrophage differentiation. *Oncogene* 1999; **18**: 6488–6495.

38 Yang JS, Nam HJ, Seo M, Han SK, Choi Y, Nam HG *et al.* OASIS: online application for the survival analysis of lifespan assays performed in aging research. *PLoS ONE* 2011; **6**: e23525.

Supplementary Information accompanies this paper on the Oncogene website (http://www.nature.com/onc)